# *Effect of polymer architecture on Curcumin encapsulation and release from PEGylated polymer nanoparticles: toward a drug delivery nano-platform to the CNS*

Jean-Michel Rabanel[1,2 ÿ], Jimmy Faivre[1 ÿ], Ghislain Djiokeng Paka[3], Charles Ramassamy[3,], Patrice Hildgen[2,] Xavier Banquy,[1, *]

[1] *Canada Research Chair on Bio-inspired materials and Interfaces*
*Faculté de Pharmacie, Université de Montréal,*
*C.P. 6128, Succursale Centre-ville, Montréal, Québec, H3C 3J7, Canada*

[2] *Laboratoire de Nanotechnologie Pharmaceutique,*
*Faculté de Pharmacie, Université de Montréal,*
*C.P. 6128, Succursale Centre-ville, Montréal, Québec, H3C 3J7, Canada*

[3] *INRS-Institut Armand-Frappier*
*531, Boulevard des Prairies*
*Laval, Québec H7V 1B7, Canada*

[*] *Corresponding author:*
*Faculté de Pharmacie, Université de Montréal, Montréal, Qc Canada*
*Fax : (+1) 514-343-2470; Tel. (+1) 514-343-2102;*
*E-mail : xavier.banquy@umontreal.ca (X Banquy)*

[ÿ] *These authors contributed equally to this work*

## Graphical Abstract

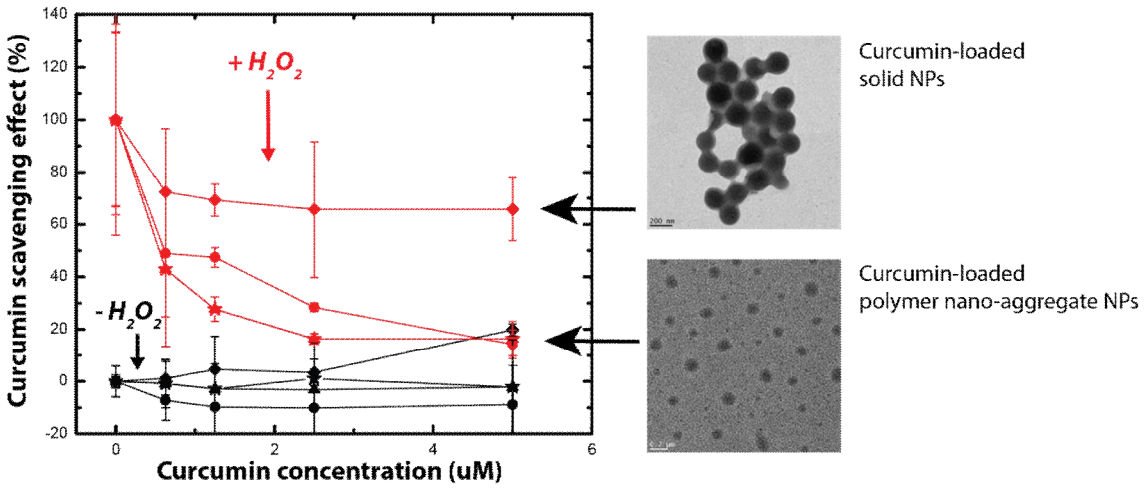

**Abstract**

We developed a nanoparticles (NPs) library from poly(ethylene glycol)-poly lactic acid comb-like polymers with variable amount of PEG. Curcumin was encapsulated in the NPs with a view to develop a delivery platform to treat diseases involving oxidative stress affecting the CNS. We observed a sharp decrease in size between 15 to 20 % w/w of PEG which corresponds to a transition from a large solid particle structure to a ñmicelle-likeò or ñpolymer nano-aggregateò structure. Drug loading, loading efficacy and release kinetics were determined. The diffusion coefficients of curcumin in NPs were determined using a mathematical modelling. The higher diffusion was observed for solid particles compared to ñpolymer nano-aggregateò particles. NPs did not present any significant toxicity when tested *in vitro* on a neuronal cell line. Moreover, the ability of NPs carrying curcumin to prevent oxidative stress was evidenced and linked to polymer architecture and NPs organization. Our study showed the intimate relationship between the polymer architecture and the biophysical properties of the resulting NPs and sheds light on new approaches to design efficient NP-based drug carriers.

**Key words**: poly(lactic); poly(ethylene glycol), comb-polymer, nanoparticle, micelle-like, nanoaggregate, curcumin, toxicity, ROS, CNS.

## 1. Introduction

Neurodegenerative disorders (NDD) are an increasing burden for the health systems and amongst all NDD, Alzheimer disease (AD) represents the most common disease. Besides the complexity of the pathophysiology of these diseases, NDD and AD are also particularly difficult to treat due to the limited permeability of the blood-brain barrier (BBB). Indeed, the BBB is very efficient to prevent the entry of foreign compounds in the central nervous system (CNS), thanks to a very tight endothelial structure and the action of efflux pumps [1, 2]. Moreover, the drugs available for the treatment of AD are in limited number and are symptomatic drugs associated with unwanted peripheral secondary effects. Finally, considering the number of mechanisms involved in AD progression, delivery of compounds with pleiotropic properties is a promising strategy. For instance, several studies have pointed out that curcumin, a phyto-polyphenol with anti-oxidative, anti-inflammatory activities and low toxicity, could alter several mechanisms involved in AD such as the amyloid-beta cascade, the phosphorylation of Tau protein as well as the development of oxidative stress [3]. However, curcumin brain bioavailability is low due to its poor stability in physiological media [4] and poor permeability across the BBB [5, 6].

Curcumin encapsulation in nanocarriers has been extensively studied for different therapeutic applications, mainly in an effort to by-pass the BBB but also to improve its solubility limitation and chemical instability. Liposomes, micelles, lipids or albumin particles [3, 7-9], as well as polyester-based carriers [5, 10] and poly(cyanoacrylate) based carriers [11] have been proposed to deliver curcumin and other substances to the CNS. Curcumin encapsulated in PLGA NPs showed an increased accumulation in CNS tissues compared to free curcumin [12].

Nanoparticle-mediated efficient uptake of active substances into the CNS represents the new field of nanomedecine with great challenge and could represent a major breakthrough in the

management of different CNS disorders. Although several proofs of concept have been put forward, the main goal stays elusive, mainly for reasons linked to the dose levels actually delivered, accumulation of polymeric material in the host, more complex cellular environment and interspecies differences between models [13]. Amongst those reasons, one that has been clearly underestimated is the structural properties of the particle. The relationships between the polymer architecture and the resulting NP structural organization are still a matter of debate in spite of several decades of research. In the area of pharmaceutical polymeric nanocarrier, diblock polymers are the most commonly used polymers to form NPs [14, 15]. On the other hand, few systematic studies focusing on establishing the relationship between the polymer architecture and the performances of the nano-carriers in term of encapsulation efficiency, release profile and more generally drug efficacy, are available.

The ability of PEGylated NP to penetrate into the brain tissue through the BBB is still a matter of debate. It is well established that drug carriers must be PEGylated in order to circulate for an extended period of time in the blood stream and to provide enough time to the different transport mechanisms to improve NP brain accumulation. ñNakedò NPs are usually rapidly opsonized resulting in an increase of liver uptake and macrophage elimination. This strongly decreases their distribution in other organs and tissues, including brain tissues. The influence of PEGylation on the BBB crossing mechanisms is not well documented yet. It has been reported that PEGylated poly(alkylcyanoacrylate) NP penetrate the brain tissues more efficiently than any other nanoformulation using other surface modifications [14, 16]. The specific crossing of a non-compromised BBB (in absence of brain injury or inflammation creating gaps between endothelial cells.) involves passage through a layer of endothelial cells via endocytosis, lysosomal escape and exocytosis on the brain parenchyma side [17, 18]. Modification of NP surface properties using polymers such as Poloxamer®, polysorbates and PEG have been shown to favour adsorption of

serum ApoE on the NP surface [13]. ApoE can be used as a targeting ligand allowing translocation of the NP across the BBB via the ApoE receptor present on endothelial cell surfaces [7]. The effect of PEG surface densities and PEG surface organization on BBB crossing efficiency is not well documented. To our knowledge, systematic exploration of these parameters is yet to be conducted.

Considering the often opposite properties a NP has to display for a successful clinical outcome [19], the development of innovative polymer architectures is necessary to maximize the efficacy of delivery to the CNS. We previously developed a library of polymers based on a comb-like architecture exhibiting a backbone of polylactic acid with pendant polyethylene glycol chains. We showed that by systematically varying the amount of PEG in the polymer, we were able to control the NP structure from solid particles to soft, polymer nano-aggregate or ñmicelle-likeò particles [20].

In this work, we used this library of PEG-*g*-PLA polymers to prepare nano-vectors loaded with curcumin. The effect of polymer architecture on the structure of the particle, drug encapsulation efficiency, drug loading, the drug release and its modeling taking in account curcumin degradation, were studied. The suitability of these NP for antioxidant delivery was evaluated on a neuronal cell line. This work represents the first step toward the development of an efficient drug delivery system to the CNS. Moreover, our library of NP with a systematic variation of PEG content and PEG surface densities may provide a tool to explore the role of PEG in the NP crossing of the BBB.

## 2. **Materials and Methods**

## 2.1 Materials

The synthesis of the different polymers used in this study was described elsewhere [20]. Briefly, random copolymerization of D,L-dilactide and benzyl glycidyl ether (BGE) was performed by ring-opening polymerization catalyzed by stannous 2-ethyl hexanoate ($SnOct_2$). The BGE/lactic acid ratio was varied from 0.5 to 3 % to yield PLA chains with different densities of benzyl pendant moities. Alcohol pendant groups were deprotected by catalytic hydrogenation in presence of Pd/Carbon to yield OH-g-PLA. mPEG-COOH (2kD) was grafted onto OH-g-PLA polymers by acylation to yield PEG-g-PLA (polymer A and C in Figure 1). Alternatively, the mPEG-COOH chains were grafted by esterification in presence of dicyclohexylcarbodiimide (DCC) [21]. The diblock synthesis (PEG-b-PLA, polymer B in Figure 1) was performed as follow: mPEG-OH 2kD was used as a macro-initiator during the ring-opening polymerization of dilactide in presence of $SnOct_2$ as previously described [20]. Polymer properties obtained from GPC and $^1$H-NMR are summarized in Table 1.

All chemicals were from Sigma-Aldrich (Oakville, ON Canada) unless otherwise stated in the text. Solvents were from Fisher Scientific (Fisher Canada, ON). Curcumin was obtained from AK scientific (AK Scientific, Union city, CA, USA). SK-N-SH cells which are human neuroblastoma cells, were from ATCC (Manassas, VA, USA), Cell culture media, minimal essential medium Eagle (MEM), fetal bovine serum, penicillin, streptomycin, and sodium pyruvate were obtained from Sigma-Aldrich (Oakville, ON, Canada). LDH and Tox-8 detection kits were from Sigma-Aldrich (Oakville, ON Canada).

## 2.2 NPs fabrication and purification

NP batches were prepared by nanoprecipitation. Briefly, 60 mg of PEGylated polymer were dissolved in 3 ml acetone. For drug-loaded NP batches, curcumin was added to the organic phase

at a determined curcumin/polymer ratio (from 0 to 20 % w/w). The organic phase was slowly injected with a syringe pump (Kent Scientific Corp. Torrington, CT, USA) at a rate of 1mL/min with a 26G needle in 15 mL of PBS 10mM (pH 7.4) placed in a 25 ml beaker. The aqueous phase was kept under constant stirring (530 rpm) with a magnetic agitator during the injection of the organic phase.

NPs were purified by centrifugation on a tabletop centrifuge (Multi RF centrifuge, Thermo Electron Corp. Needham heights MA, USA) to remove eventual large debris, aggregates and precipitated non-encapsulated curcumin (5 min at 5000 rpm). Supernatant was finally dialyzed against PBS during 2 h in a regenerated cellulose membrane bag, with a cut-off of 6-8000 Da (SpectraPor, Spectrum Laboratories, Rancho Dominguez, USA) to remove organic solvent residuals as well as small non-precipitated polymer chains. NPs were stored in a dark container at 4°C or were used immediately after preparation. Residual amount of non-encapsulated curcumin in solution are rapidly degraded in the aqueous phase during NP suspension storage and are thus not contributing to observed biological properties.

### 2.3 NPs characterization

- ***Size measurements.*** The NPs size was measured by Dynamic Light Scattering (DLS) on a Zetasizer Nano-ZS (Malvern Instruments, Worcester, UK). Three measurements of 15 (10 seconds) runs were performed at 25°C and averaged.
- ***Zeta potential measurements.*** NPs suspended in 1 ml of PBS 0.1 X pH 7.4 were placed in a disposable folded capillary cell to measure ɛ on a Malvern Zetasizer (Malvern, Worchester, UK) in triplicate.
- ***Loading efficiency (LE) and drug loading (DL).*** LE and DL were assessed by UV/Vis spectrophotometry (MBI Lab equipment, Montréal, CA) using a standard curve of curcumin in

dichloromethane (DCM) at $\lambda_{max}$=419 nm. Briefly, 1 mL of NPs was lyophilized and precisely weighted, then dissolved in DCM. Dissolved polymers effect on absorbance was found not significant. Curcumin concentration was then measured by UV/Vis. LE and DL were calculated using equations (Eq. 1) and (Eq. 2) respectively:

$$LE = \frac{\text{weight of curcumin in NPs}}{\text{initial weight of curcumin}} \times 100 \quad (Eq.1)$$

$$DL = \frac{\text{weight of curcumin in NPs}}{\text{weight of NPs}} \times 100 \quad (Eq.2)$$

NP exact weights were adjusted for the presence of PBS salts in samples.

### 2.4 Differential Scanning Calorimetry (DSC)

DSC experiments were performed on blank and loaded NPs. A mass of about 5 mg of freeze-dried (blank or drug-loaded) NP was disposed in crimped aluminum pan. DSC analysis were performed under nitrogen flow from -40°C to 80°C at 10°C $min^{-1}$, hold for 1 minute and cooled at a rate of 20°C $min^{-1}$ to -40°C and reheated to 80°C at 10°C $min^{-1}$. First run was analyzed for NP samples using TA instruments Universal Analysis 2000, version 4.5A (TA Instruments ï Waters LLC, USA).

### 2.5 **Transmission electronic microscopy (TEM)**

*Sample preparation for TEM* Diluted NP suspension in MilliQ® water at a concentration of about 1 to 2 mg/ml were deposited on a carbon film of 400 square mesh copper grids (Electron Microscopy Sciences, Hatfield, PA USA). The volume of the droplet was about 2 to 4 µl. The droplet was allowed to sit for 5 minutes before excess of liquid was drained-out with filter paper. Grids were allowed to dry in air for 1-2 hours before image acquisition. No staining procedure was introduced.

*TEM imaging* TEM image acquisition was done in bright field mode on a JEM-2100F, Field Emission electron microscope (Jeol Ltd, Tokyo, Japan) equipped with a sample holder cooled by liquid nitrogen (Gatan inc. Warrendale, Pittsburg, PA, USA). The grids were maintained at -170$^{o}$C throughout the acquisition with a temperature controller (Smart Set Model 900 Cold Stage controller; Gatan inc. Warrendale, Pittsburg, PA, USA). The grids were introduced in the microscope column under vacuum. Liquid nitrogen was added to the sample holder and temperature recorded. The sample was exposed to the electron beam only after the temperature had reached -170$^{o}$C. The acceleration voltage was set at 200 kV. Images were digitally recorded at a low electron dose to prevent damage to the heat-sensitive particles (current densities were between 5 and 15 pA/cm$^2$).

### 2.6 Drug release studies

Release studies were carried out in triplicate using the dialysis bag method at 37°C in an orbital shaker. In brief, 3 mL of NPs suspension were placed in a dialysis bag (Cellulose ester membrane, cut-off 100 kDa, Spectrum Laboratories, Rancho Dominguez, USA) and then, immersed in 30 mL of 10 mM PBS (pH 7.4) supplemented with 50 mM Sodium Dodecyl Sulfate (SDS) to increase curcumin solubility in the release medium and insure sink conditions. Ascorbic acid (ASA) was also added to the medium (25µM) to minimize curcumin oxidation. At each time-point, 3 mL of external media were removed and replaced by fresh solution. The curcumin solution was dosed by UV/Vis spectrophotometry according to a standard curve of curcumin in a 10 mM PBS/SDS/ASA buffer at $\lambda_{max}$=422 nm.

### 2.7 Cytotoxicity studies

Cytotoxicity studies were carried out as described previously [22] with some modifications described here. Briefly, SK-N-SH cells were maintained in MEM, supplemented with 10% v/v FBS, 100 U/mL penicillin, 100 g/mL streptomycin, and sodium pyruvate (1mM) in a humidified

incubator at 37 °C with 5% $CO_2$. Cells were grown to 80% confluence and then seeded in multi-well cell culture plates.

*Cytotoxity assays*. SK-N-SH cells were plated at a density of $2.0 \times 10^4$ cells/well in 96-well plates and incubated for 24 h at 37 °C. Cells were then treated with either free curcumin, blank NP or curcumin-loaded NP in presence or absence of $H_2O_2$ (250µM) (n=3). Curcumin solutions are prepared as follow to avoid precipitation: A stock solution of 200 µM is prepared by the solubilisation of 1 mg of curcumin in 0.5 mL of Ethanol and the volume is completed with 13 mL of PBS. This stock solution was used to prepare solution of free curcumin in all biological tests. Control experiments (not shown in this study) had previously showed that this procedure had not effect on biological results [10]. Preparation of blank or curcumin-loaded NP, characterized for their size, mass concentration and drug loading, were diluted to obtain 0.25 to 1 µM curcumin equivalent concentration in either blank or curcumin-loaded NP samples. Practically, the same concentration of particles was used in experiments involving blank and loaded NPs. This allows for a direct comparison and control of NP effects, to be distinguished from curcumin effects. Cell death and survival were measured 24 h after the treatment using the cytotoxicity detection kit-LDH and the survival detection kit Tox-8 (Resazurin-based) respectively. The kits were used following the manufacturerôs instructions. Values obtained from controls, untreated cells, were considered as 100% of proliferation for Resazurin-based assays. For cell mortality assays (LDH-based assays) and ROS level determination (DCF-DA assays), values obtained from controls untreated cells were considered as 0% effect on mortality, while values obtained from control untreated cells exposed to 250µM $H_2O_2$ were considered as 100% effect on mortality. Raw results from treated cells were thus normalized based on these controls to allow a direct comparison of the different treatments and account for cell-assays variability from plate to plate.

### 2.8 Effect of Reactive Oxygen Species (ROS) and reactive nitrogen species (RNS).

Effect of NPs on intracellular ROS and RNS as well as protective effect of blank and drug loaded NPs on neuronal cells in presence or absence of 250 µM $H_2O_2$ were assessed by following the oxidation of 2ô,7ô ï dichlorofluorescin diacetate (DCF-DA) a non-fluorescent, cell permeable dye that, upon hydrolysis by intracellular esterase, reacts with ROS/RNS to produce a highly fluorescent compound, 2ô, 7ô ï dichlorofluorescein (DCF), which is trapped inside the cells. Briefly, SK-NSH cells ($2 \times 10^4$/well) were plated into 96-well plates. After 24 hours, cells were exposed with 10 µM DCF-DA for 20 min and treated with either free curcumin, blank NP or curcumin-loaded NP for 1 h in presence or absence of $H_2O_2$. At the end of the treatment, cells were then washed with PBS containing $Ca^{2+}$/$Mg^2$ and the fluorescence was determined with the excitation/emission filters at 485/ 535 nm using a Synergy HT multi-detection microplate reader (BioTek Instruments, Inc, Highland Park, Winooski, Vermont USA).

ROS level determination (DCF-DA assays), values obtained from controls untreated cells were considered as basal level (0%), while values obtained from controls untreated cells exposed to 250µM $H_2O_2$ were considered as the 100% effect on ROS levels. Raw results from treated cells were thus normalized based on these controls to allow a direct comparison of the different treatments and account for cell-assays variability from plate to plate.

### 2.9 Statistical analysis

Multiple groups comparison of cell-based assays were performed with a one-way Anova on SigmaStats® (Systat Software Inc.) using the Holm-Sidak method. Significance level was set at $p<0.05$.

## 3. Results and discussion

### *3.1 Polymer characteristics*

The polymers used in this study, noted as PEG-*g*-PLA throughout the text, are comb-like polymers composed of a PLA backbone on which PEG chains are grafted. In addition to PEG-*g*-PLA polymers, PLA polymer bearing no PEG chain (OH-*g*-PLA) as well as a PEG-*b*-PLA di-block polymer were included to the study in order to better characterised the effect of PEG content and architecture. The polymersô architectures are presented in Figure 1. The properties of the polymer used in this study are listed in Table 1.

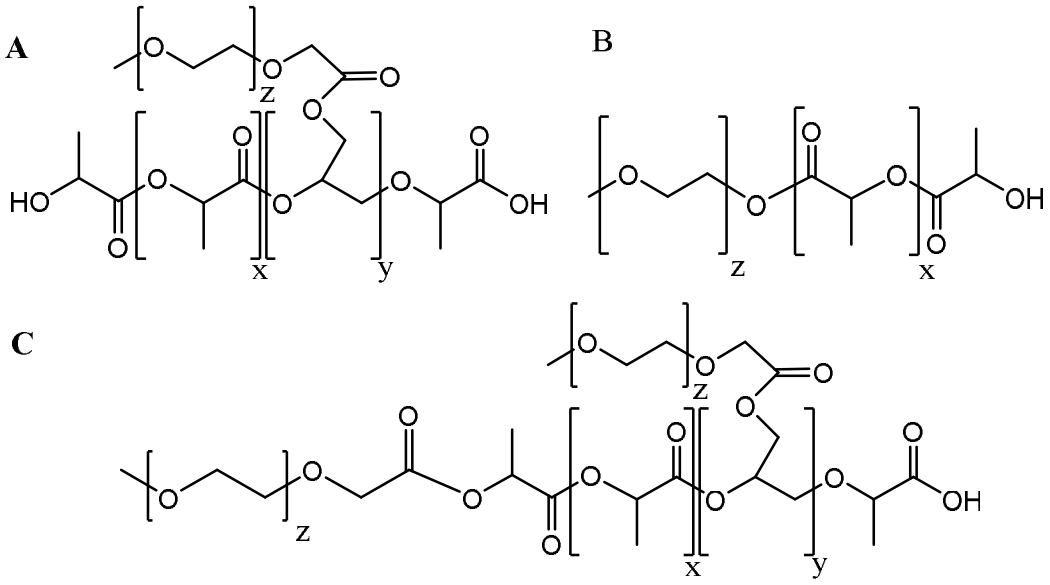


**Figure 1.** Structures of the polymers used in this study. **(A)** PEG-*g*-PLA; **(B)** PEG-PLA di-block polymer, **(C)** PEG-*g*-PLA with a terminal PEG graft. (z= 45; y : 0.5-2.5/100 LA monomers)

**Table 1.** Polymer properties (from [20])

| *Polymer* | *Molar Mass $M_w$* | | *%PEG* | *Structure* |
|---|---|---|---|---|
| | *PLA (g/mol)* | *PEG (g/mol)* | *(% w/w)* | *See figure 1* |
| *OH-g-PLA* | *23 990* | - | *0* | - |
| *PEG-PLA* | *23 000* | *2 000* | *6* | *B* |
| *PEG8%-g-PLA* | *28 300* | *2 000* | *8* | *A* |
| *PEG12%-g-PLA* | *40 300* | *2 000* | *11.6* | *A/C* |
| *PEG15%-g-PLA* | *33 890* | *2 000* | *14.9* | *A/C* |
| *PEG20%-g-PLA* | *19 820* | *2 000* | *19.9* | *C* |
| *PEG25%-g-PLA* | *23 990* | *2 000* | *24.9* | *C* |
| *PEG38%-g-PLA* | *28 300* | *2 000* | *37.9* | *C* |

PEG chains ($M_w$=2 000 g/mol) were grafted on a PLA backbone of $M_w$ å25 000 g/mol (Table 1). The resulting polymers exhibited a PEG content varying from 8 to 37.9 %w/w (Table 1). The choice of the PLA backbone size was determined by its appropriate short degradation time [23]. Numbers of grafted PEG chains on polymeric chain were determined by $^1$H-NMR [20].

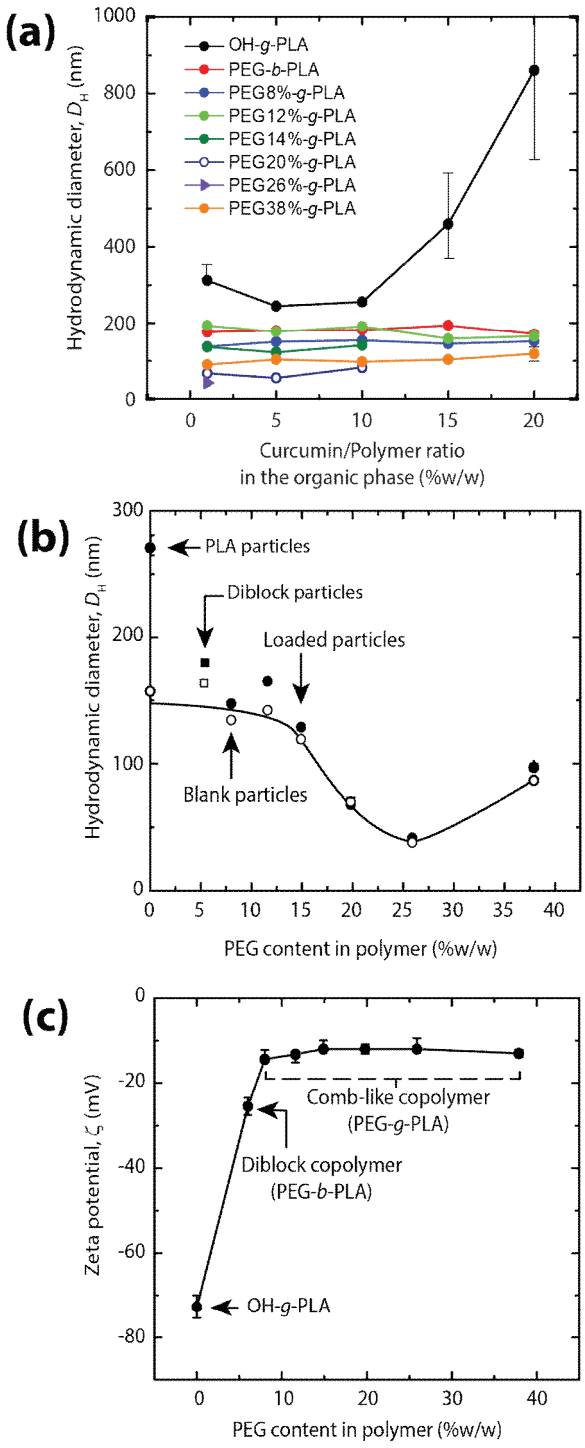


**Figure 2.** Particle hydrodynamic diameter as a function of: **(a)** initial curcumin/polymer content in the organic phase (% mass); or **(b)** PEG content. **(c)** Zeta potential of the NPs as a function of polymer PEG content. In (a) and (b) some error-bars are not showing since they are smaller than the symbol used.

*3.2 NP preparation and characterization*

NP made with different curcumin contents (% w/w ratio curcumin/polymer varying from 0 to 20%) in the organic phase were prepared by nanoprecipitation and characterized. Except for NPs prepared with OH-*g*-PLA, curcumin-loaded NP showed no significant size differences compared to blank NPs (Fig. 2a). This observation is in agreement with Budhian *et al.* who encapsulated haloperidol in PLA-based nanoparticles and found that NPs mean diameter was independent of the initial haloperidol content [24]. Similar observations were made by Gou *et al.* in a work involving encapsulation of curcumin in a micellar system [25].

Fig. 2b shows the evolution of the NPs hydrodynamic diameter as a function of PEG content in the polymer (% w/w PEG/PLA). NPs size was found to be constant and independent of PEG content up to 15 % w/w PEG. Above this value, a sharp decrease in size is observed to about 50 nm at 25% w/w PEG/PLA. Afterwards, NPs hydrodynamic diameters increase again slowly, up to 100 nm with increasing PEG content (Fig. 2b). This increase could be due to the higher surface PEG chain density resulting in stretched PEG chains and increase in particle hydrodynamic diameter, as predicted by De Gennesô theory [26]. Similar observations were reported for this polymer library previously for blank NPs [20].

OH-*g*-PLA NPs (NPs made of polymer before it has been modified by PEG grafting) showed a different behaviour when prepared with a ratio of 15% w/w curcumin/polymer. The colloidal system was instantaneously destabilized, resulting in a drastic NP hydrodynamic diameter increase. It can be hypothesized that, when OH-*g*-PLA is used, curcumin precipitation occurred much faster than the polymer precipitation and particles formation. As a result, curcumin precipitation drags down polymer chains leading to the complete destabilization of the system. On the other hand, PEG side chains in di-block and comb-like copolymers contribute to the nano-suspension stabilization.

NPs zeta potential was also studied as a function of PEG content in polymer (Fig. 2c). OH-*g*-PLA NPS exhibited a strongly negative zeta potential of -75 mV providing a strong electrostatic repulsion in aqueous solution between PLA particles. The presence of PEG chains on PLA backbone decreases drastically zeta potential to a value of -15 mV. However this decrease remained independent of the polymer PEG content. NPs produced with the diblock polymer exhibited a zeta potential slightly more negative compared to NPs obtained with comb-like polymers. The dramatic decrease in zeta potential with increased PEG content has been also reported by Gref *et al.* [27]. Such phenomenon has been attributed to the displacement of the shearing plane far away from NPs surface by the presence of PEG chains around the NPs, hiding the carboxylic groups present in the PLA core. However, low electrostatic repulsions for PEG-*g*-PLA NPs are counterbalanced by the increased steric hindrance around PEGylated NPS which guarantees a stable colloidal suspension. The difference between diblock and PEG-*g*-PLA zeta potentials can be explained by the smaller PEG/PLA ratio used in the diblock copolymer (Table 1) which decreases the PEG density around corresponding NPs. Another explanation can be related to the structural organization of comb polymer preventing PLA terminal COOH to be exposed at the NP surface [20].

Morphology of blanks and drug-loaded particles was examined by TEM. To prevent damage or deformation of the NPs, TEM grids were maintained at -170$^{o}$C during image acquisition. No structural differences were noticeable between blank and curcumin-loaded particles (Fig. 3). Between 0 and 12-15 % w/w of PEG, NPs appear to belong to a particulate (solid particle) regime and the size of the hydrophobic core determined the NPs size. Between 0 and 12-15 % w/w of PEG, NPs appear as solid particles. NPs with a 8% PEG content (Figure 3C and D), as well as control NPs prepared from pure PLA or OH-*g*-PLA, (Figure S2) exhibit a large particle size and a homogeneous core.

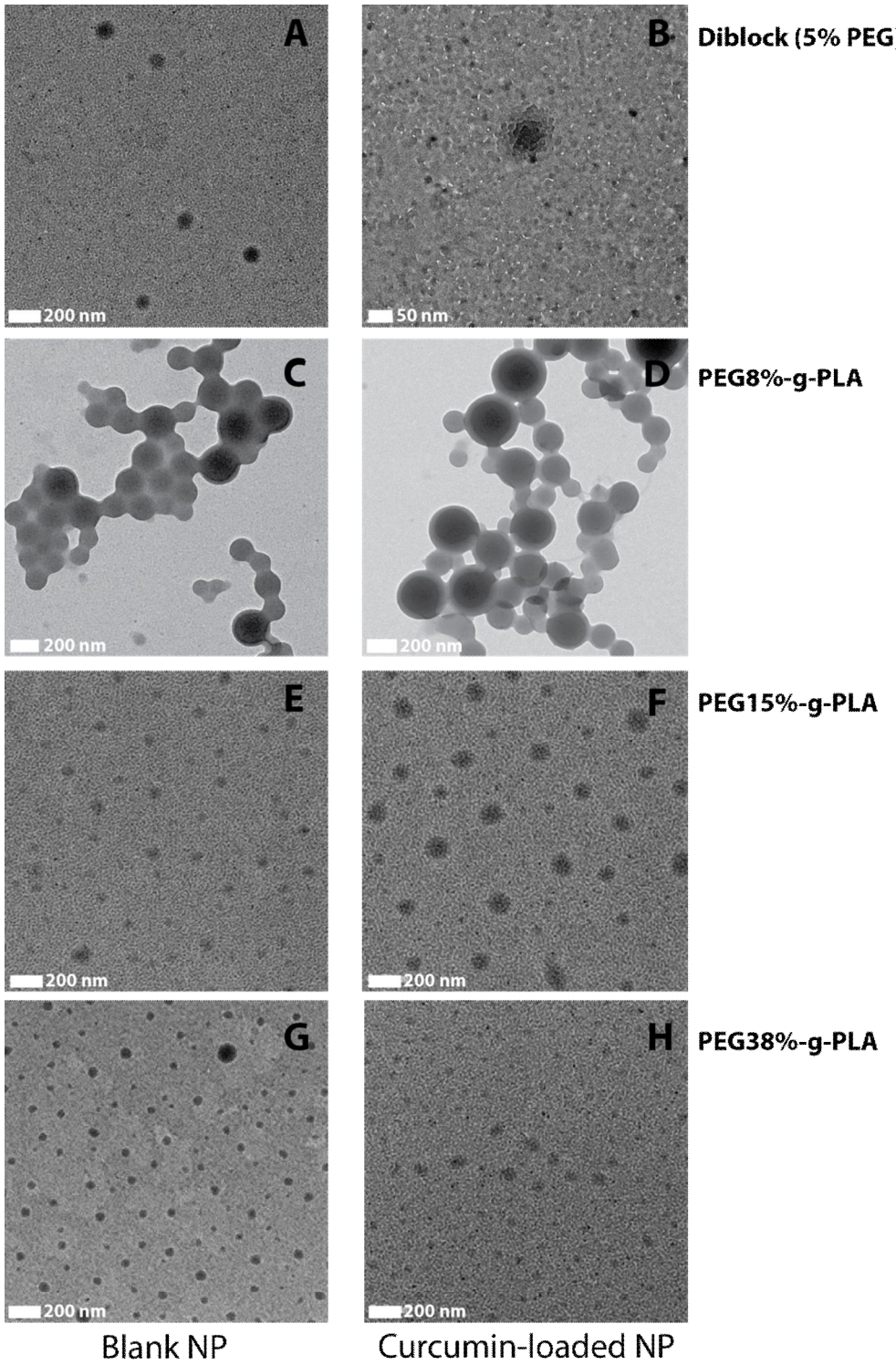


**Figure 3.** Representative TEM images of the NPs under study. On left panels: blank particles; on the right panel: curcumin-loaded particles. Acquisition at 15 000 X, except (B) acquisition at 25 000 X. (A and B), Diblock PEG-*b*-PLA NPs; (C and D), PEG8%-*g*-PLA NPs; (E and F) PEG15%-*g*-PLA NPs; (E and F) PEG38%-*g*-PLA NPs

Beyond 15% of PEG content, it was hypothesized that nanocarriers switch to a ñmicellar-likeò or ñpolymer nano-aggregateò structural organization, a kinetically micellar frozen system (Fig 3E,F,G,H) in response to increased PEG content per polymeric chain [20]. All polymer nano-aggregate particles appeared round shaped and non-aggregated.

The changes in particle size previously observed by DLS were confirmed by TEM. Particles with PEG content below 12 % w/w were found to be much larger (>100 nm) than those with higher PEG content (<100m). Interestingly, our results show that the transition from solid NPs to polymer aggregate NPs depends only on the PEG content in the polymer and its architecture but not on the molecule encapsulated in the NPs, since no difference was observed between curcumin-loaded-NP and blank NP. Noteworthy, the morphology of diblock NP appears more spherical and less polydispersed than particles made from comb polymer of similar PEG content. The dramatic change in size and particle morphology from solid polymeric NPs to soft polymeric aggregates is not only related to polymer PEG content but also to polymer architecture as PEG-*b*-PLA diblock with PEG content about 6% adopt a soft particle morphology as seen in TEM (Fig. 3A and B)).

*3.3 Curcumin encapsulation*

Systematic quantification of the loading efficiency (LE) and the drug loading (DL) of curcumin in the NPs were conducted to correlate these properties with the architecture and PEG content of the polymers. Fig. 4 shows the evolution of the LE and DL as a function of the initial curcumin/polymer ratio in the organic phase.

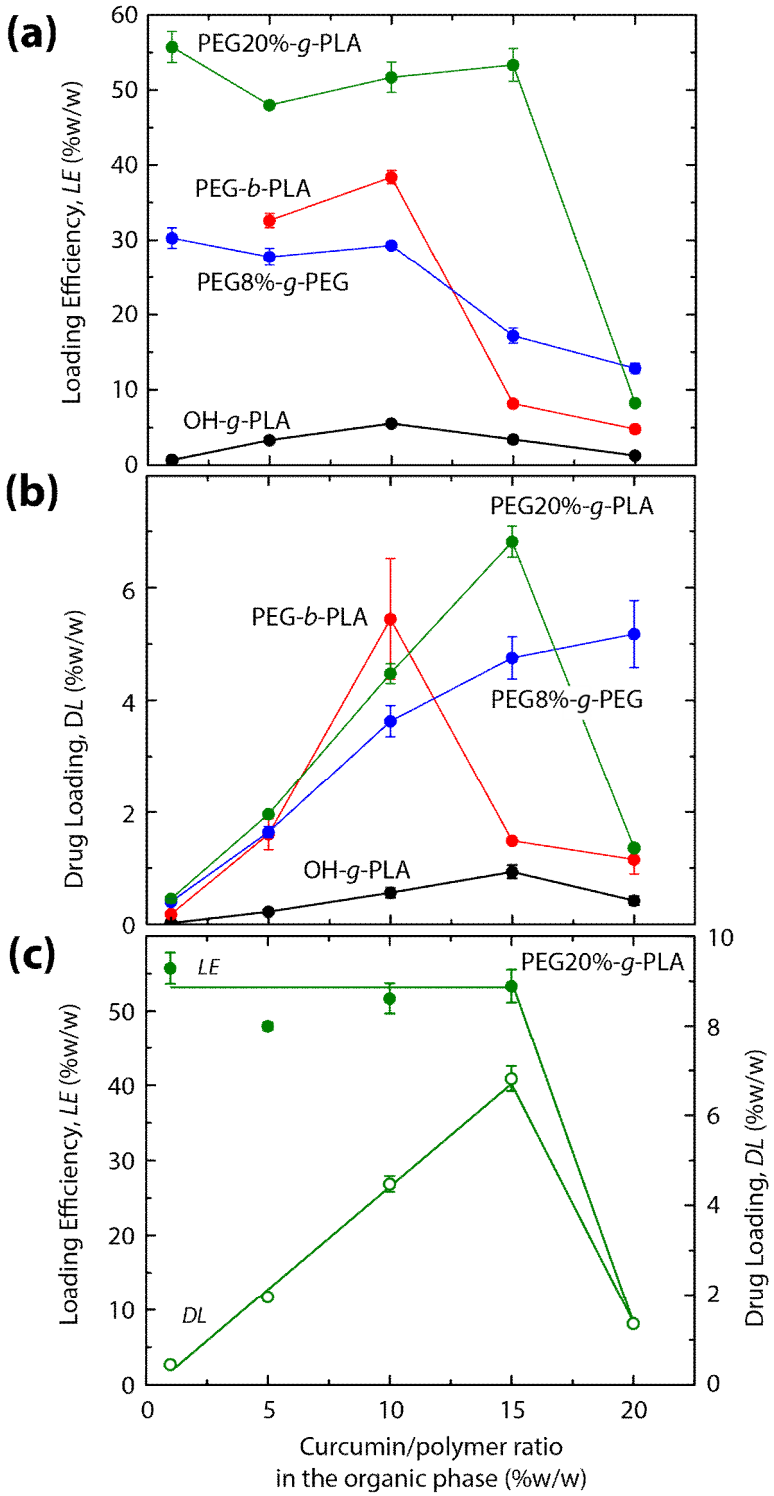


**Figure 4**. Optimization of encapsulation process: **(a)** Loading efficiency (LE) as a function of curcumin/polymer ratio; **(b)** Drug loading (DL) as a function of curcumin/polymer ratio; **(c)** Direct comparison of Loading efficiency and Drug loading (DL) as a function of curcumin/polymer ratio for ñpolymer nano-aggregateò particle made of PEG20%-*g*-PLA.

LE was found to vary between nearly 0% for OH-*g*-PLA NPs, 20% for solid particles and up to 50% for the polymer nano-aggregate NPs. For DL, values spread out from 0% for OH-*g*-PLA to 5% for polymer nano-aggregate NPs. As a result, these NPs exhibiting the highest PEG content were found to have the highest values of LE and DL. As shown in Fig. 4, LE exhibited a plateau before drastically decreasing to values lower than 10 % at 20% w/w curcumin/polymer (Fig. 4a). At the same time, the DL first increased up to a maximum value, which depends on the polymer PEG content, before decreasing (with the exception of PEG8%-*g*-PLA (Fig. 4b). Budhian *et al.* reported a similar behaviour for the encapsulation of haloperidol in PLA based-NPs [24, 28]. The authors explained this phenomenon as the result of the drug/polymer interactions. By increasing the curcumin initial content, the encapsulation yield (LE) remains at the maximum efficiency as indicated by the plateau, and the drug loading (DE) increases until it reaches its maximum, which can be considered as the drug maximum solubility in the polymeric matrix (Fig. 4c). Beyond this limit, LE drastically decreases due to drug saturation in the NPs. It follows that curcumin concentration in the aqueous phase increases and reaches rapidly its saturation in solution and precipitates. The non-encapsulated curcumin precipitate drags down polymer chains, destabilizing the system and resulting in a dramatic decrease in DL [29].

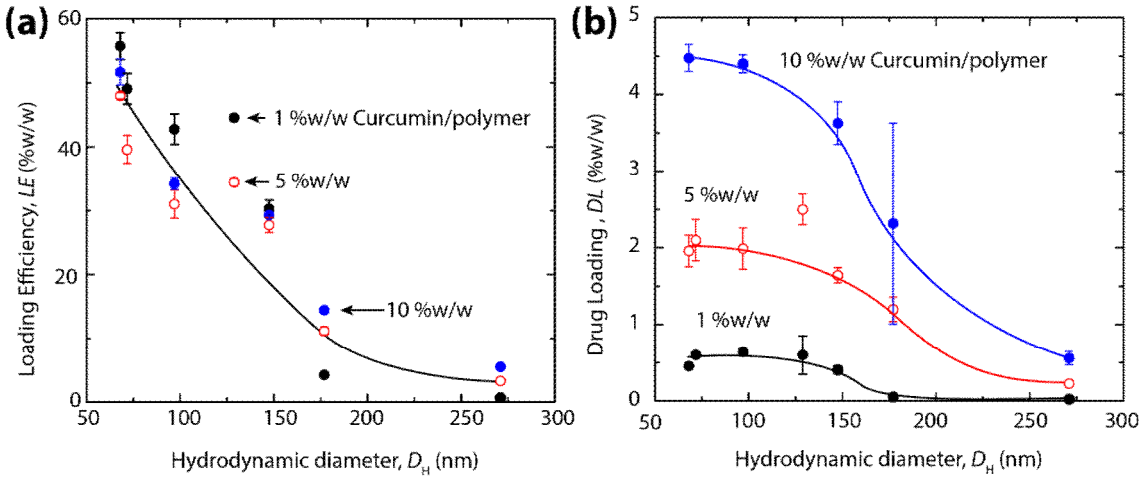


**Figure 5.** Evolution of **(a)** Loading Effciency (LE) and **(b)** Drug Loading (DL) as a function of the NPs hydrodynamic diameter.

The NPs ability to encapsulate curcumin was also correlated to NPs hydrodynamic diameter (Fig. 5). The highest values of LE and DL were obtained for the smallest nanocarriers with a LE of about 50% (Fig. 5a) and a DL of about 5% (Fig. 5b). Both LE and DL decrease with the particle size to reach values close to 0% for NPs produced with OH-*g*-PLA polymer (i.e. PLA chain with hydroxyl branching points along the polymer backbone). Noteworthy, the size of particle is also directly correlated to PEG content. Although curcumin is poorly soluble in PEG, NP PEG content could play a role in LE and DL values. For instance, PLGA nanoparticles prepared with PEO-PPG, an amphiphilic molecule known to cover the surface of the NPs, were shown to be more efficient to encapsulate curcumin than ñbareò PLGA NPs [30].

The relationship between polymer architecture, PEG content and encapsulation properties can be summarize as follow: The increase of PEG content is related to an increase in LE. Noteworthy PEG-*b*-PLA with a 6% PEG content showed a higher LE than PEG8%-*g*-PLA comb polymer pinpointing the role of polymer architecture. The maximum DL is about 4-6% regardless of the PEG content. For each polymer, the maximum DL is obtained at different drug/polymer ratio as seen in Fig 4b. This may be related to two parameters: 1) solubility of curcumin in polymer, mainly the hydrophobic PLA backbone chains present in variable amount in each polymer; 2) the relative precipitation speed between the polymer chains and curcumin as discussed above, and finally 3) a retention effect of curcumin inside the NP due to the hydrophilic PEG layer.

The encapsulation efficiency depends on drug/polymer interactions [29], the structural organization of the NP and the preparation process of the NP. During the nanoprecipitation process, a key factor is the relative rate of precipitation of the hydrophobic drug and the polymer. If the rates of precipitation of the two species are equal, they will form homogeneous particles while large differences between rates will force the selective precipitation of each component and

disfavor the encapsulation of the drug. The rate of precipitation of the polymer is mainly controlled by its PEG content, being lower at high PEG content.

Regarding the role of the interactions between the drug and the polymer, in our case, the strong affinity of the drug to the PLA backbone of the polymer is due to hydrophobic forces. As shown in our previous study [20], NPs obtained from polymers of high PEG content tend to exhibit more hydrophobic central cores compared to lightly PEGylated NPs. As PEG content increases in the polymer, it becomes more segregated to the surface of the NPs during the fabrication process which allows, to a certain extent, to improve drug solubility in the core of the NPs. On the other hand, the increased density of the PEG layer on the surface of the NP impedes to some extend curcumin release during the encapsulation process during release experiments as observed in our experimental data. These points are further discussed in light of release and diffusion study results (Section 3.4).

*3.4 Curcumin release and stability studies*

Release studies were carried out using the same initial curcumin content in NPs over 1 week. Because quantity of encapsulated curcumin in pure PLA NP was so small, it was not possible to dose any release with the detection method used (UV absorbance). This formulation was removed from the release studies. Fig. 6a shows representative release profiles of curcumin from NPs suspended in PBS supplemented with SDS and ascorbic acid at 37°C. Acid Ascorbic was used as an anti-oxidant to prevent curcumin degradation [30] and SDS was added to increase the solubility of curcumin in the aqueous media and ensure sink conditions [31]. Release profiles followed trends independently of the PEG content in the NPs (Fig. 5a). During the first 24 h of release, a fast increase of curcumin concentration is observed followed by an exponential decrease over more than 48 h to reach the detection limit of curcumin released. The apparent

decrease of curcumin concentration is due to its degradation by oxidation besides the presence of ascorbic acid. Curcumin is known to be unstable in several aqueous media with a degradation of 90% in 30 min in PBS 100mM [4, 32].

In order to quantify curcumin degradation during the release studies, degradation kinetics were quantified in the same media than release studies, at two different concentrations. In these conditions, the degradation kinetics showed a first order degradation rate with a constant $k_d$ equal to $0.01h^{-1}$ (see Fig. S1) and a degradation of 50% after 3 days at 37°C. With the purpose to obtain more insights on the effect of polymer architecture and PEG content on curcumin release, a simple diffusion-degradation model was fitted to the experimental data (Eq. 3) [33].

$$\frac{Mt}{M\infty} - \exp(-k_d.t) - \frac{6}{\pi^2}\sum_{n=1}^{\infty}\frac{1}{n^2}.\exp\left(-\frac{D.n^2.\pi^2.t}{r^2}\right) \quad \text{(Eq. 3)}$$

where $M_t$ and $M^{\infty}$ are the released mass of curcumin at time $t$ and time infinite respectively, $D$ is the diffusion coefficient of curcumin in the NPs and $r$ is the NP radius (see Table S1 for the list of calculated modelling parameters). The first term in the equation accounts for the degradation of curcumin while the second term models the Fickian diffusion of the drug from spherical particles. [34] We ensured that the assumptions of the diffusion model, namely: 1) Perfect sink conditions of curcumin in release media, 2) Solubility concentration higher than drug concentration within the NP matrix, 3) No swelling, degradation, surface and bulk erosion of the copolymer during the release timeframe, were verified experimentally. As mentioned already, sink conditions were fulfilled thanks to SDS addition which increases curcumin solubility in the release media [31]. TEM pictures were examined and DSC analyses were performed to identify the presence of any crystallized areas in the NPs, which could suggest that curcumin concentration was higher than its solubility in the NP. It was found that the polymeric matrix was homogenous and no fusion peak appeared on the DSC thermograms, suggesting curcumin

solubilisation in the polymeric matrix (data not shown). Moreover, encapsulated curcumin has no apparent effect on polymer thermal properties ($t_g$) and thus their organization within the NPs (Fig. S3). Right after the release experiments, absence of polymer degradation and bulk erosion in curcumin-loaded NP material were verified by GPC and DLS size measurements respectively (data not shown) supporting a model for which drug diffusion is the limiting factor of the release. This is not unexpected as it has been reported previously that erosion plays a minor role in drug release from diblock polyesters-PEG NPs. [35]

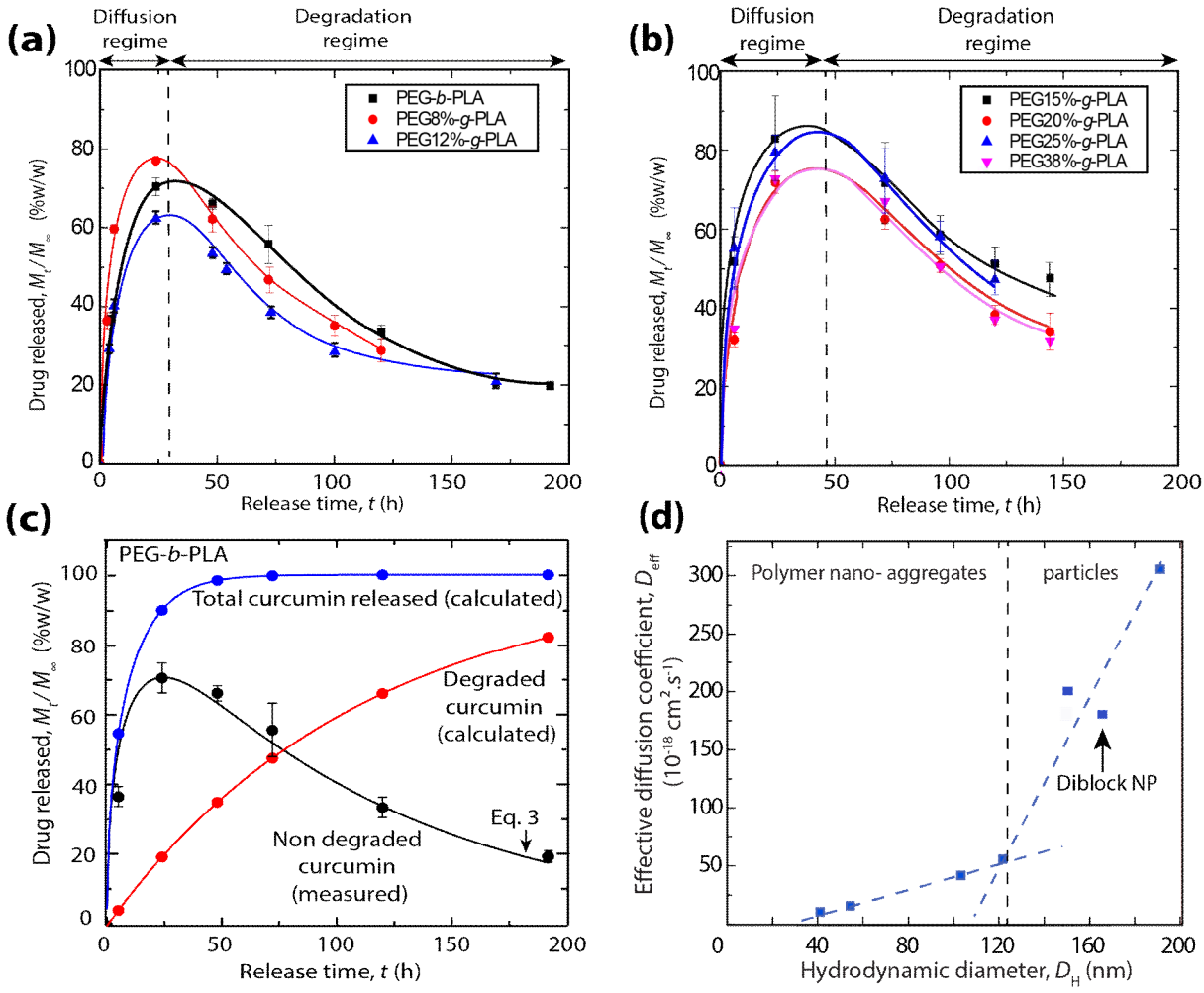


**Figure 6.** Representative release profiles of curcumin at 37°C from **(a)** solid NP and **(b)** ñmicelle-likeò or ñpolymer nano-aggregateò NPs. **(c)**. Modelling of curcumin release from diblock NPs, showing the evolution with time of the purely diffusive and drug degradation contributions. **(d)**.Dependence of the drug diffusion coefficient *D* obtained using Eq. 3 on NP size.

Equation 3 was used to obtain the diffusion coefficient of curcumin in the NPs. The diffusion coefficient (*D)* was set as the sole free parameter. It was then possible to estimate the theoretical curcumin release without its degradation (Fig. 6c top curve). Results revealed that the diffusion coefficient in the largest NPs was about 10 times higher than in the smallest NPs (Fig. 6d). One possible explanation in the difference between the diffusion constant of the different particle batches could be linked to the surface density and thickness of PEG outside layer creating a diffusion barrier to the very hydrophobic curcumin molecule in the smaller particles. Peracchia *et al.* were the first to report a slowing down of the drug release from polymeric NP having a surface PEG coating. Moreover, they showed that this effect was surface PEG density and PEG chain length dependent [35]. Another explanation could come from the internal structure differences between particles of different size. For instance, porosity may be higher in large particle compared to nanoparticles favouring hydration of the particle core and release of their content [36]. This hypothesis is also in agreement with Budhian *et al.* who measured a higher diffusion coefficient of haloperidol encapsulated in 1.3 µm PLA/PLGA micro-particles (without PEG chains corona) compared to 450 nm NPs and to 220 nm NPs [24]. On the other hand, diffusion through the polymer matrix can be favoured by low polymer $t_g$ or by a molecularly dispersed drug as seen by DSC for all the NPs tested.

The PEG content and polymer architecture play a role not only in the determination of NP structure but on drug encapsulation and release. The drug release profiles (Fig 6a and b) and diffusion constants as calculated during release modelling show two regimes, related in part to the size of the NP (Fig 6d). They are also related to the NP morphologies observed, i.e. solid particles (NP made with comb-polymers with low PEG content) and polymer nano-aggregate particles (NP made of comb-polymers with high PEG content and diblock polymer) (see Fig. S4, plotting $D_{eff}$ against polymer PEG content). Relatively large but ñsoftò diblock NPs appear in an

intermediate position in term of drug diffusion (Fig. 6d), highlighting the role of polymer architecture.

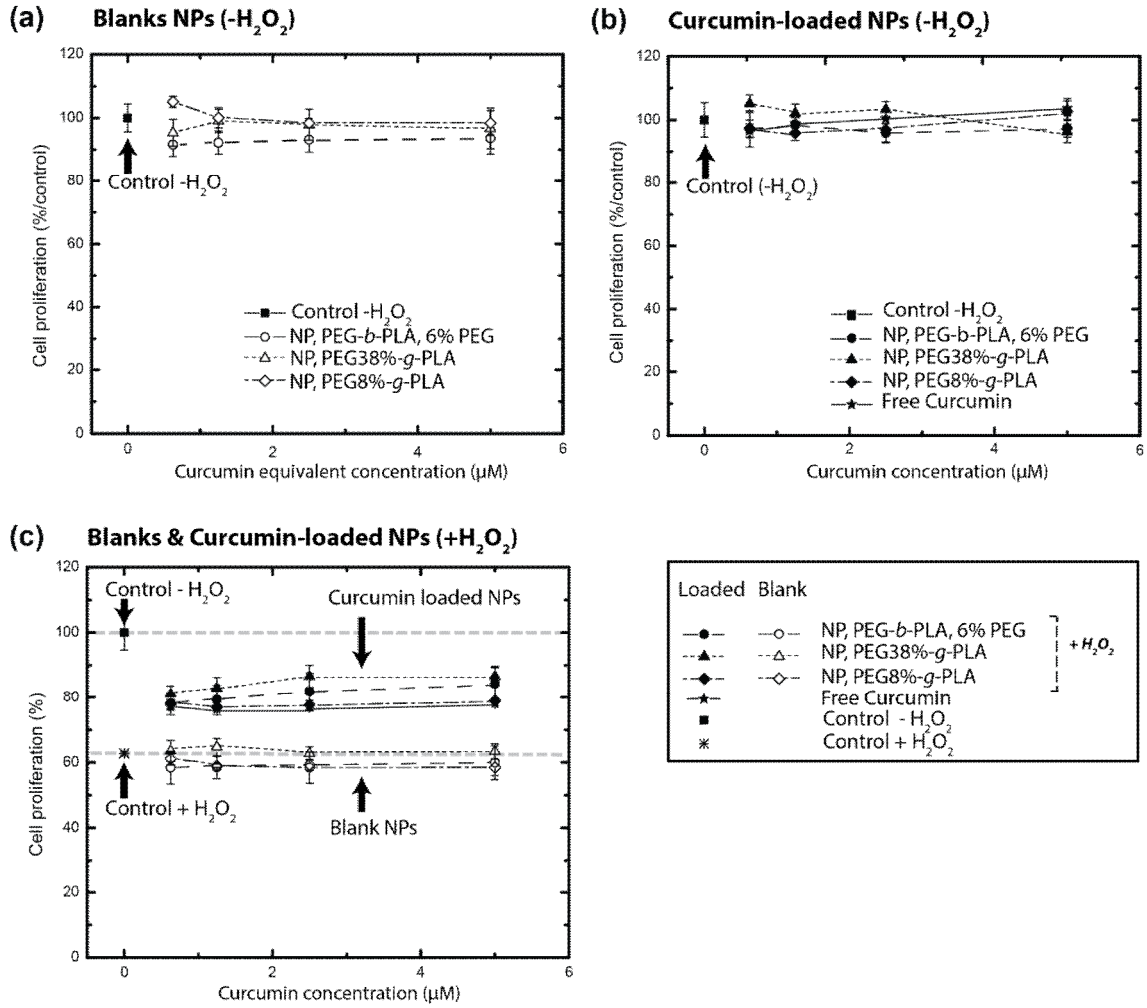


**Figure 7.** Cytotoxicity as assessed by the Rezasurin ï cell viability assay of blank NPs **(a)** and curcumin-loaded NPs **(b)** on SK-N-SH neuronal cells. Panel **(c)** shows Rezasurin ï cell proliferation assay in presence of $H_2O_2$ (250µM) in the medium. Particle concentrations were adjusted to curcumin concentrations (or equivalent for blank NP): For blank NP, abscises are expressed in curcumin concentration for comparison purpose. Practically, an equivalent quantity of drug-loaded NP in blank NP are added for each curcumin concentration levels

*3.5 In vitro studies.*

*3.5.1 Cytotoxicity studies*

To test the protective properties of the curcumin-loaded NPs against oxidative stress, we performed two separate tests using resazurin test and LDH assay respectively. Resazruin test allows the monitoring of cell proliferation and metabolism, while LDH assay monitors change in cell membrane integrity.

Di-block NP (5% PEG w/w), comb-polymer PEG-*g*-PLA at 8 and 38% PEG content (%w/w) were tested in cell culture model as representative of solid particle and nano-aggregate NP batches. Resazurin test, a cell proliferation assay confirmed the absence of adverse effects on cell proliferation and metabolism in the range of tested concentrations for both blank and curcumin-loaded particles (Fig. 7a and b). In the presence of hydrogen peroxide (Fig. 7c), cell survival was reduced by 40% and 20% with blank NPs and Cur-NP, respectively.

These results demonstrate that encapsulated curcumin was efficient to protect cells against hydrogen peroxide oxidative stress. But on the other hand there is only a partial preservation of cell proliferation and metabolism upon addition of curcumin-loaded NP. Moreover, we found no clear dose-response relationship showing an increase of cell proliferation and metabolism upon addition of higher curcumin dose. This result could be put in perspective with the curcumin release kinetic in regard on the condition of the assays performed here, as discussed in the following section.

LDH assays did not reveal any evidence of cytotoxicity for blank (Fig. 8a) and curcumin-loaded NPs (Fig. 8b) of any batches of NPs on neuronal cell line SK-N-SH. These tests demonstrate that, independently of their size, polymer architecture and PEG content, the NPs under study are clearly not cytotoxic to neuronal cells.

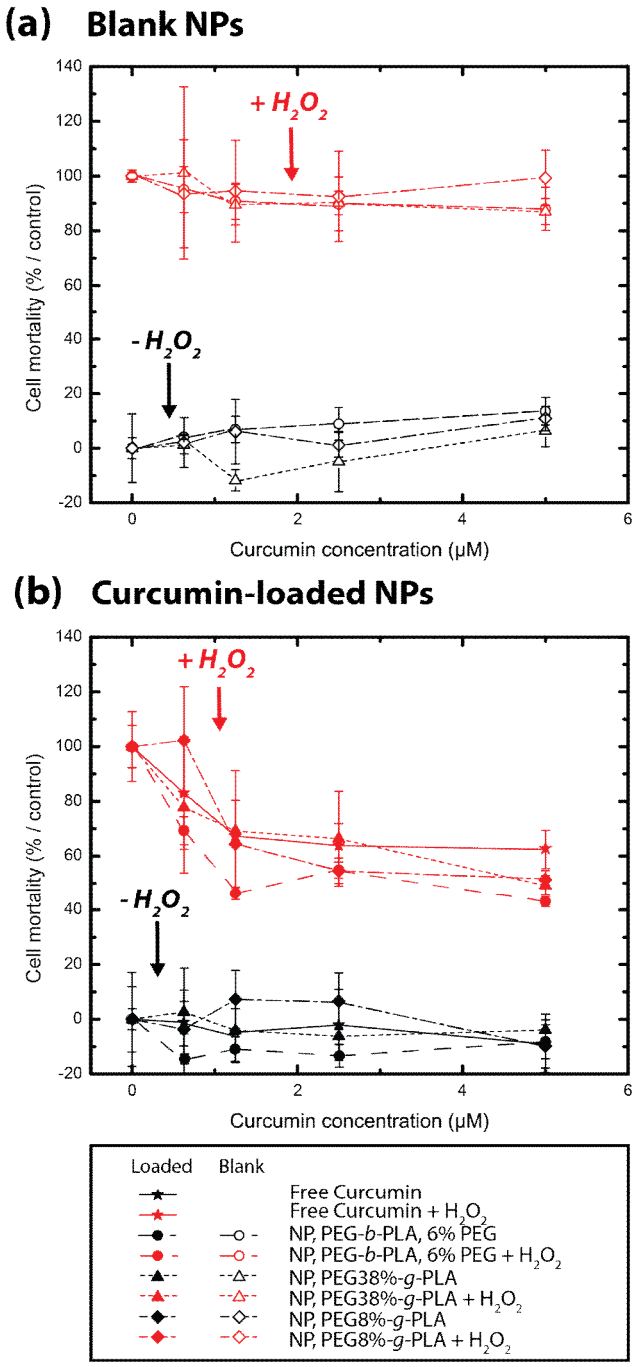


**Figure 8.** Relative LDH release assay (cell mortality assay). **(a)** Controls experiments with blank NP **(b)** Curcumin-loaded NP with (symbol in red) or without (symbol in black) addition of $H_2O_2$ in the medium. The level of LDH release induced by $H_2O_2$without treatment has been considered as 100%. For blank NP, abscise is expressed in curcumin concentration for comparison purpose. Practically, an equivalent quantity of drug-loaded NP in blank NP are added for each curcumin concentration levels

In assays involving addition of $H_2O_2$, as expected, an increase in cell mortality (measured by LDH released in the medium) is observed in controls experiments (Fig. 8). Noteworthy, NP toxicity was not exacerbated by induction of oxidative stress upon addition of $H_2O_2$ in the medium (Fig. 8a). The addition in the media of the blank NP did not affect the release of LDH in the media (Fig. 8a). This indicates that NP themselves are not able to counteract cell mortality induced by hydrogen peroxide. This is an important control as seemingly non-specific effect of blank NP has been reported and attributed to the properties of NP to carry serum proteins to the cells in culture and induce change in cell proliferation and mortality [37].

On the other hand, curcumin-loaded NP appeared to have a significant effect under the tested conditions (Fig. 8b), particularly for the di-block NP (5% w/w PEG). However the magnitude of the effect is comparable to free curcumin added to the media (no statistical differences between the groups, $p>0.05$).

*3.5.2 Reactive Oxygen Species production and inhibitions*

The direct measurement of intracellular ROS was performed by DCF fluorescence dosage. The control experiments with blank NP show little or no effect on intracellular ROS concentration (Fig. 9a). No statistically significant scavenging effect was observed for blank particles (upper curves in Fig. 9a). On the other hand, curcumin-loaded NPs showed a dose-response decrease on intracellular ROS levels (Fig. 9b). At the highest tested concentrations, di-block loaded NP and polymer nano-aggregate loaded particles were able to restore ROS level to a level comparable to untreated cells, while loaded solid NPs (PEG8%-*g*-PLA) appear to be less efficient to counteract the elevation of ROS (Fig. 9b). The di-block and nano-aggregate NP were found to be as effective as free curcumin, as no statistically significant difference between free curcumin, curcumin-loaded di-block or polymer nano-aggregate particles were found (Fig. 9b). The difference in effects of each curcumin-loaded NPs batches on ROS levels (Fig. 9b, may arise

from the size of the NP, the rate of release, site of release (extra or intracellular release) and the possible interaction with cells.

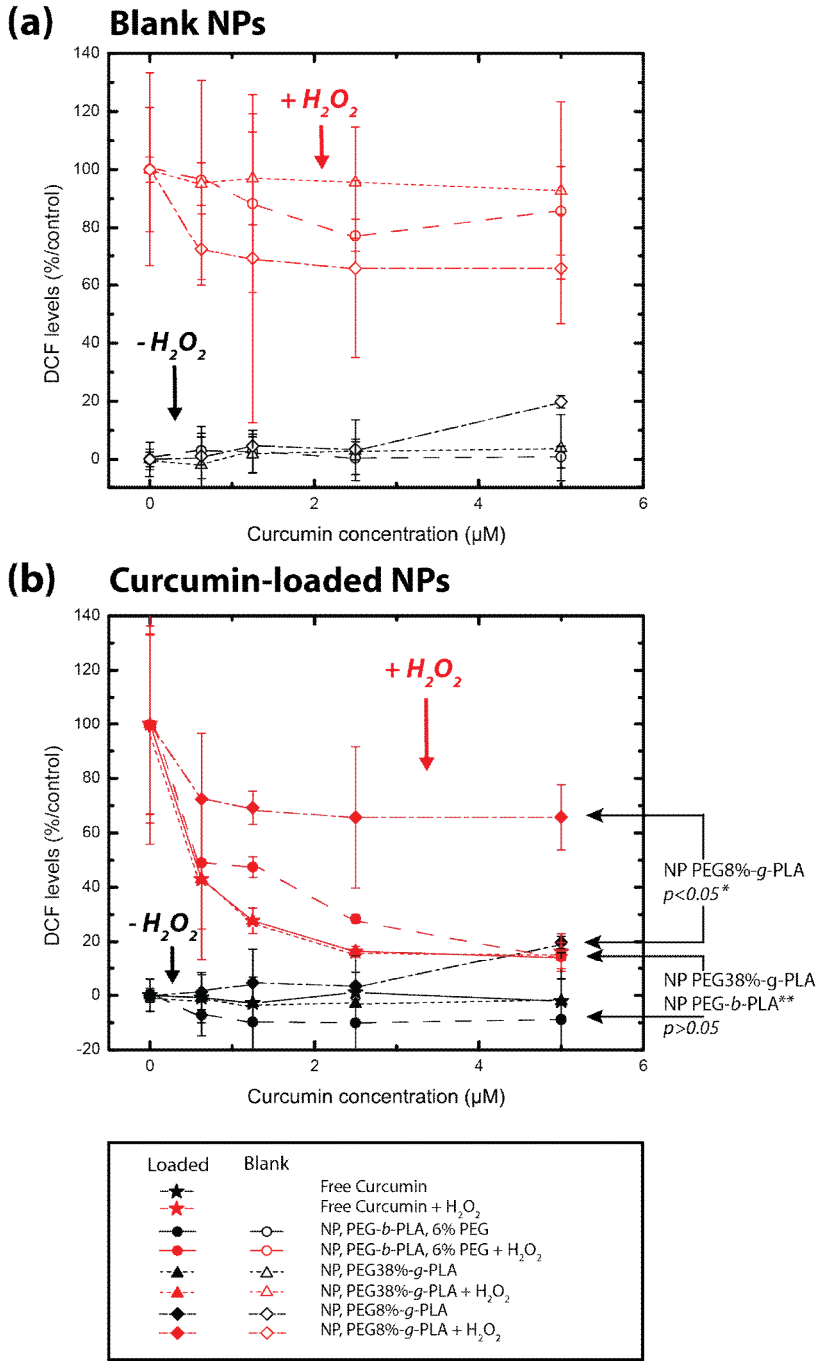


**Figure 9.** Relative intracellular levels of ROS **(a)** Control experiments with blank NP (blank NP concentration equivalent to concentration of curcumin-loaded NP) without addition of $H_2O_2$ (black symbol) or with $H_2O_2$ (250µM added to the medium). (red symbol); **(b)** Treatment experiments: Level of ROS as determined by DCF detection in response to treatment with curcumin-loaded NP without addition of $H_2O_2$ (black symbol) or with $H_2O_2$ (250µM added to the

medium). (red symbol) The level of ROS induced after $H_2O_2$ addition without treatment has been considered as 100%

All these results should be correlated to the kinetic of drug release by these NPs. Figure 6a shows a superior release for high PEG content NP compared to low PEG content NP. A faster release of curcumin should translate into greater scavenging effect considering the conditions of these experiments. Within the time frame of the experiment (1 h) the curcumin dose encapsulated into the NP is only partially released (about 25 to 35% of the dose as seen in Fig. 6a and 6b), limiting its scavenging effect. Moreover the released content is exposed to degradation in the medium and the cytosol, decreasing the effective dose at a given time point.

The polymer architecture controls the drug release (as seen in section 3.4 ñCurcumin release and stability studiesò) and modulates exposure of curcumin to ROS (Fig 9). In spite of PEG-*b*-PLA NPs and PEG38%-*g*-PLA NPs differences in hydrodynamic diameters and PEG content, they appear as effective to decrease intracellular ROS levels. On the other hand, PEG-*b*-PLA and PEG8%-*g*-PLA NPs with similar size and similar PEG content show large difference in scavenging efficacy.

*3.5.3 Polymeric NP toxicity*

Induction of oxidative stress effects by NPs has been reported mostly for silica or metal oxides NPs (inorganic) as well as carbon nanotubes and carbon particulates generated by pollution. The type of stress reported can go from damages to proteins by reactive NPs surface, to the generation of oxygen reactive species or the depletion of the medium from antioxidant molecules [38]. Even if these effects were reported for organic NPs [10, 22, 39], few studies on polymeric NP toxicity address this issue. In the conditions of the test, however, we did not detect any effect of di-block and polymer nano-aggregate NPs, either blank or drug-loaded on the generation of intracellular ROS (Fig. 9b). A minor effect on ROS level is observed for solid NP

(NP made from PEG8%-*g*-PLA) at the higher dose (5µM curcumin or equivalent) as seen on Fig. 9a and 9b. This effect on ROS levels is not correlated with cell mortality as shown in Figure 8a and 8b depicting LDH release in the medium and its origin is unknown at this time.

### *3.5.4 Discussion summary*

This work showed the intimate relationship between the polymer architecture, block composition and the biophysical properties of the resulting NPs. We previously identified a transition of physio-chemical properties of NP made of PEG branched PLA around 15% PEG content (w/w) [20]. In this study, drug encapsulation and release properties are found to also follow this trend as shown by encapsulation results (Fig. 4), release profiles (Fig. 6) and notably biological effects (Fig. 9). The increase of PEG content is related to an increase in LE (Fig. 4). On the other side, PEG-b-PLA diblock with a 6% PEG content showed a higher LE than PEG8%-g-PLA comb polymer illustrating the role of architecture. The drug release profiles (Fig. 6a, 6b) and diffusion constants show two regimes, related in part to the size of the NP (Fig. 6d) and the NP morphologies observed, i.e. solid particles (NP made with comb-polymers with PEG content <15%) and polymer nano-aggregates (NP made of comb-polymers with PEG content >15% and diblock polymer). Relatively large but ñsoftò diblock NPs appear in an intermediate position in term of drug diffusion coefficient (Fig. 6d), highlighting again the role of polymer architecture on the NPs inner structure and fluidity. Finally, polymer architecture controls and modulates exposure of curcumin to ROS and thus antioxidant activity. Diblock polymer and high PEG content comb polymers appeared to be the most efficient to reduce oxidative stress (Fig 9). In this study we have limited our investigation to copolymers of PEG 2kD chains and hydrophobic PLA backbones of almost constant molecular weight. The information we gathered from the comb-like polymers library in comparison to diblock PEG-b-PLA and PLA only suggest that both PEG content and polymer architecture (i.e. the position at which PEG chains are

attached to the hydrophobic backbone) play a role in the NP properties. PEG content appears determinant for particle size, while architecture seems determinant for the structural organization of the particle (solid NPs vs nanoaggregates) This aspect was extensively discussed in a previously published work describing the polymer synthesis and characterization of blank NPs [20]. All together these results contribute to shed light on new approaches to design efficient polymer-based drug carriers.

## 4. Conclusion

A library of PEGylated grafted PLA polymers were used in order to establish correlations between physico-chemical properties of the NPs and curcumin encapsulation and release properties of the said particles. A structural transition, described previously for several particle properties, located around 15 % PEG content (% w/w) and suggesting a transition from a solid particle regime to a micelle-like behaviour, was also found for release properties of curcumin. This transition initially identified in term of structural properties, seems related to changes in encapsulation and release properties of loaded curcumin as well.

Release studies and mathematical modelling of curcumin taking into account degradation was designed to fit the experimental data and to estimate the real release. Cell-based assays support the non-toxicity of the particles to neuronal cell lines. Moreover, oxidation scavenging effects of curcumin-loaded NP show the potential benefit of those formulations for oxidative-stress-related CNS diseases. Di-block and micelle like NP were found as effective as free curcumin in the condition of the experiments. However, NP formulation may prove to be superior on long term effect thank to their protective effect on curcumin and slow release properties. This aspect will be address in future studies. PEGylated polymeric particle may also have therapeutic benefit by themselves in AD by their effect on amyloid aggregation [40]. This assumption has to be clarified by further studies in our system. Lastly, another point to be

explored is the optimization of the blood brain barrier crossing of different formulation with the view to develop *in vivo* assays.

## Appendix A. Supplementary material

Supplementary data: TEM images, Curcumin degradation kinetics, table of modelling parameters and DSC results. This material is available free of charge via the Internet at http://www.sciencedirect.com


## Acknowledgments

JMR wish to thank the ñ*Fonds de Recherche du Québec ï Nature et Technologie*ò (Québec, Canada) and the Faculty of pharmacy of the Université de Montréal for doctoral fellowships. XB acknowledges the support of Canada Research chair program of the government of Canada, PH acknowledges FRQ-NT funding and CR support from ñ*Chaire de recherche Louise et André Charron sur la maladie dôAlzheimer*ò of INRS-Institut Armand-Frappier, Laval, Québec, Canada. Technical assistance of Johanne Habr in encapsulation studies as well as the help of Soudeh F. Tehrani in polymer synthesis are acknowledged. TEM imaging was performed at the Centre de Caractérisation Microscopique des Matériaux ($CM^2$) of the École Polytechnique (Montréal, QC, Canada) with the help of Jean-Philippe Massé.


## References


[1] M.M. Patel, B.R. Goyal, S.V. Bhadada, J.S. Bhatt, A.F. Amin, Getting into the Brain: Approaches to Enhance Brain Drug Delivery, CNS Drugs, 23 (2009) 35-58 10.2165/0023210-200923010-200900003.

[2] J.M. Rabanel, V. Aoun, I. Elkin, M. Mokhtar, P. Hildgen, Drug-loaded nanocarriers: passive targeting and crossing of biological barriers, Curr. Med. Chem., 19 (2012) 3070-3102.

[3] J.K. Sahni, S. Doggui, J. Ali, S. Baboota, L. Dao, C. Ramassamy, Neurotherapeutic applications of nanoparticles in Alzheimer's disease, J. Control. Release, 152 (2011) 208-231.

[4] Y.-J. Wang, M.-H. Pan, A.-L. Cheng, L.-I. Lin, Y.-S. Ho, C.-Y. Hsieh, J.-K. Lin, Stability of curcumin in buffer solutions and characterization of its degradation products, J. Pharm. Biomed. Anal., 15 (1997) 1867-1876.

[5] A. Mathew, T. Fukuda, Y. Nagaoka, T. Hasumura, H. Morimoto, Y. Yoshida, T. Maekawa, K. Venugopal, D.S. Kumar, Curcumin loaded-PLGA nanoparticles conjugated with Tet-1 peptide for potential use in Alzheimer's disease, PLoS ONE, 7 (2012) e32616.
[6] A. Belkacemi, S. Doggui, L. Dao, C. Ramassamy, Challenges associated with curcumin therapy in Alzheimer disease, Expert Rev. Mol. Med., 13 (2011) null-null.
[7] A. Zensi, D. Begley, C. Pontikis, C. Legros, L. Mihoreanu, S. Wagner, C. Buchel, H. von Briesen, J. Kreuter, Albumin nanoparticles targeted with Apo E enter the CNS by transcytosis and are delivered to neurones, J. Control. Release, 137 (2009) 78-86.
[8] M. Taylor, S. Moore, S. Mourtas, A. Niarakis, F. Re, C. Zona, B. La Ferla, F. Nicotra, M. Masserini, S.G. Antimisiaris, M. Gregori, D. Allsop, Effect of curcumin-associated and lipid ligand-functionalized nanoliposomes on aggregation of the Alzheimer's Abeta peptide, Nanomed., 7 (2011) 541-550.
[9] L. Gastaldi, L. Battaglia, E. Peira, D. Chirio, E. Muntoni, I. Solazzi, M. Gallarate, F. Dosio, Solid lipid nanoparticles as vehicles of drugs to the brain: current state of the art, Eur. J. Pharm. Biopharm., 87 (2014) 433-444.
[10] S. Doggui, J.K. Sahni, M. Arseneault, L. Dao, C. Ramassamy, Neuronal Uptake and Neuroprotective Effect of Curcumin-Loaded PLGA Nanoparticles on the Human SK-N-SH Cell Line, J. Alzheimers Dis., 30 (2012) 377-392.
[11] R.S. Mulik, J. Mönkkönen, R.O. Juvonen, K.R. Mahadik, A.R. Paradkar, ApoE3 Mediated Poly(butyl) Cyanoacrylate Nanoparticles Containing Curcumin: Study of Enhanced Activity of Curcumin against Beta Amyloid Induced Cytotoxicity Using In Vitro Cell Culture Model, Mol. Pharm., 7 (2010) 815-825.
[12] Y.-M. Tsai, C.-F. Chien, L.-C. Lin, T.-H. Tsai, Curcumin and its nano-formulation: The kinetics of tissue distribution and bloodï brain barrier penetration, Int. J. Pharm., 416 (2011) 331-338.
[13] J. Kreuter, Drug delivery to the central nervous system by polymeric nanoparticles: What do we know?, Adv. Drug Deliv. Rev., 71 (2014) 2-14.
[14] K. Andrieux, P. Couvreur, Polyalkylcyanoacrylate nanoparticles for delivery of drugs across the bloodï brain barrier, Wiley Interdisciplinary Reviews: Nanomedicine and Nanobiotechnology, 1 (2009) 463-474.
[15] J. Hrkach, D. Von Hoff, M.M. Ali, E. Andrianova, J. Auer, T. Campbell, D. De Witt, M. Figa, M. Figueiredo, A. Horhota, S. Low, K. McDonnell, E. Peeke, B. Retnarajan, A. Sabnis, E. Schnipper, J.J. Song, Y.H. Song, J. Summa, D. Tompsett, G. Troiano, T. Van Geen Hoven, J. Wright, P. LoRusso, P.W. Kantoff, N.H. Bander, C. Sweeney, O.C. Farokhzad, R. Langer, S. Zale, Preclinical Development and Clinical Translation of a PSMA-Targeted Docetaxel Nanoparticle with a Differentiated Pharmacological Profile, Sci. Transl. Med., 4 (2012) 128ra139.
[16] P. Calvo, B. Gouritin, H. Villarroya, F. Eclancher, C. Giannavola, C. Klein, J.P. Andreux, P. Couvreur, Quantification and localization of PEGylated polycyanoacrylate nanoparticles in brain and spinal cord during experimental allergic encephalomyelitis in the rat, Eur. J. Neurosci., 15 (2002) 1317-1326.
[17] S. Wohlfart, S. Gelperina, J. Kreuter, Transport of drugs across the bloodï brain barrier by nanoparticles, J. Control. Release, 161 (2012) 264-273.
[18] H. Hillaireau, P. Couvreur, Nanocarriers' entry into the cell: relevance to drug delivery, Cell. Mol. Life Sci., 66 (2009) 2873-2896.
[19] J.-M. Rabanel, P. Hildgen, X. Banquy, Assessment of PEG on polymeric particles surface, a key step in drug carrier translation, J. Control. Release, 185 (2014) 71-87.
[20] J.-M. Rabanel, J. Faivre, S. Tehrani F, A. Lalloz, P. Hildgen, X. Banquy, Effect of Polymer Architecture on the Structural and Biophysical Properties of PEG-PLA Nanoparticles, ACS Appl. Mater. Interfaces, 7 (2015) 10374ï 10385.
[21] B. Neises, W. Steglich, Simple Method for the Esterification of Carboxylic Acids, Angew. Chem., Int. Ed. Engl., 17 (1978) 522-524.
[22] S. Doggui, A. Belkacemi, G.D. Paka, M. Perrotte, R. Pi, C. Ramassamy, Curcumin protects neuronal-like cells against acrolein by restoring Akt and redox signaling pathways, Mol. Nutr. Food Res., 57 (2013) 1660-1670.
[23] M.S. Shive, J.M. Anderson, Biodegradation and biocompatibility of PLA and PLGA microspheres, Adv Drug Deliv Rev, 28 (1997) 5-24.
[24] A. Budhian, S.J. Siegel, K.I. Winey, Haloperidol-loaded PLGA nanoparticles: Systematic study of particle size and drug content, Int. J. Pharm., 336 (2007) 367-375.
[25] M. Gou, K. Men, H. Shi, M. Xiang, J. Zhang, J. Song, J. Long, Y. Wan, F. Luo, X. Zhao, Z. Qian, Curcumin-loaded biodegradable polymeric micelles for colon cancer therapy in vitro and in vivo, Nanoscale, 3 (2011) 1558-1567.
[26] P.G. de Gennes, Polymers at an interface; a simplified view, Adv. Colloid Interface Sci., 27 (1987) 189-209.
[27] R. Gref, G. Miralles, É. Dellacherie, Polyoxyethylene-coated nanospheres: effect of coating on zeta potential and phagocytosis, Polym. Int., 48 (1999) 251-256.

[28] J. Panyam, M.M. Dali, S.K. Sahoo, W. Ma, S.S. Chakravarthi, G.L. Amidon, R.J. Levy, V. Labhasetwar, Polymer degradation and in vitro release of a model protein from poly(D,L-lactide-co-glycolide) nano- and microparticles, J. Control. Release, 92 (2003) 173-187.
[29] K. Letchford, R. Liggins, H. Burt, Solubilization of hydrophobic drugs by methoxy poly(ethylene glycol)-block-polycaprolactone diblock copolymer micelles: Theoretical and experimental data and correlations, J. Pharm. Sci., 97 (2008) 1179-1190.
[30] L. Mayol, C. Serri, C. Menale, S. Crispi, M.T. Piccolo, L. Mita, S. Giarra, M. Forte, A. Saija, M. Biondi, D.G. Mita, Curcumin loaded PLGAï poloxamer blend nanoparticles induce cell cycle arrest in mesothelioma cells, Eur. J. Pharm. Biopharm., 93 (2015) 37-45.
[31] H.H. Tønnesen, Solubility, chemical and photochemical stability of curcumin in surfactant solutions. Studies of curcumin and curcuminoids, XXVIII. , Pharmazie, 57 (2002) 820-824.
[32] S. Oetari, M. Sudibyo, J.N.M. Commandeur, R. Samhoedi, N.P.E. Vermeulen, Effects of curcumin on cytochrome P450 and glutathione S-transferase activities in rat liver, Biochem. Pharmacol., 51 (1996) 39-45.
[33] J. Siepmann, F. Siepmann, Mathematical modeling of drug delivery, Int. J. Pharm., 364 (2008) 328-343.
[34] D.Y. Arifin, L.Y. Lee, C.-H. Wang, Mathematical modeling and simulation of drug release from microspheres: Implications to drug delivery systems, Adv. Drug Deliv. Rev., 58 (2006) 1274-1325.
[35] M.T. Peracchia, R. Gref, Y. Minamitake, A. Domb, N. Lotan, R. Langer, PEG-coated nanospheres from amphiphilic diblock and multiblock copolymers: Investigation of their drug encapsulation and release characteristics, J. Control. Release, 46 (1997) 223-231.
[36] S. Sant, V. Nadeau, P. Hildgen, Effect of porosity on the release kinetics of propafenone-loaded PEG-g-PLA nanoparticles, J. Control. Release, 107 (2005) 203-214.
[37] R. Hussien, B.H. Rihn, H. Eidi, C. Ronzani, O. Joubert, L. Ferrari, O. Vazquez, D. Kaufer, G.A. Brooks, Unique growth pattern of human mammary epithelial cells induced by polymeric nanoparticles, Physiological Reports, 1 (2013) n/a-n/a.
[38] P. Møller, N.R. Jacobsen, J.K. Folkmann, P.H. Danielsen, L. Mikkelsen, J.G. Hemmingsen, L.K. Vesterdal, L. Forchhammer, H. Wallin, S. Loft, Role of oxidative damage in toxicity of particulates, Free Radic. Res., 44 (2010) 1-46.
[39] A. Aranda, L. Sequedo, L. Tolosa, G. Quintas, E. Burello, J.V. Castell, L. Gombau, Dichloro-dihydro-fluorescein diacetate (DCFH-DA) assay: A quantitative method for oxidative stress assessment of nanoparticle-treated cells, Toxicol. In Vitro, 27 (2013) 954-963.
[40] D. Brambilla, R. Verpillot, B. Le Droumaguet, J. Nicolas, M. Taverna, J. Kona, B. Lettiero, S.H. Hashemi, L. De Kimpe, M. Canovi, M. Gobbi, V. Nicolas, W. Scheper, S.M. Moghimi, I. Tvaroska, P. Couvreur, K. Andrieux, PEGylated nanoparticles bind to and alter amyloid-beta peptide conformation: toward engineering of functional nanomedicines for Alzheimer's disease, ACS Nano, 6 (2012) 5897-5908.

# Supplementary Material

## *Effect of Polymer Architecture on Curcumin Encapsulation and Release from Pegylated Polymer Nanoparticles: Toward a CSN Drug Delivery Nano-platform*

*Jean-Michel Rabanel[1,2], Jimmy Faivre[1], Ghislain Djiokeng Paka[3], Charles Ramassany[3], Patrice Hildgen[2], Xavier Banquy,[1,*]*

[1] *Canada Research Chair on Bio-inspired materials*
*Faculté de Pharmacie, Université de Montréal,*
*C.P. 6128, Succursale Centre-ville, Montréal, Québec, H3C 3J7, Canada*

[2] *Laboratoire de Nanotechnologie Pharmaceutique,*
*Faculté de Pharmacie, Université de Montréal,*
*C.P. 6128, Succursale Centre-ville, Montréal, Québec, H3C 3J7, Canada*

[3] *Chaire de recherche Louise et André Charron sur la maladie d'Alzheimer*
*INRS-Institut Armand-Frappier, 531, Boulevard des Prairies*
*Laval, Québec H7V 1B7, Canada*

[*] *Corresponding authors: xavier.banquy@umontreal.ca*;

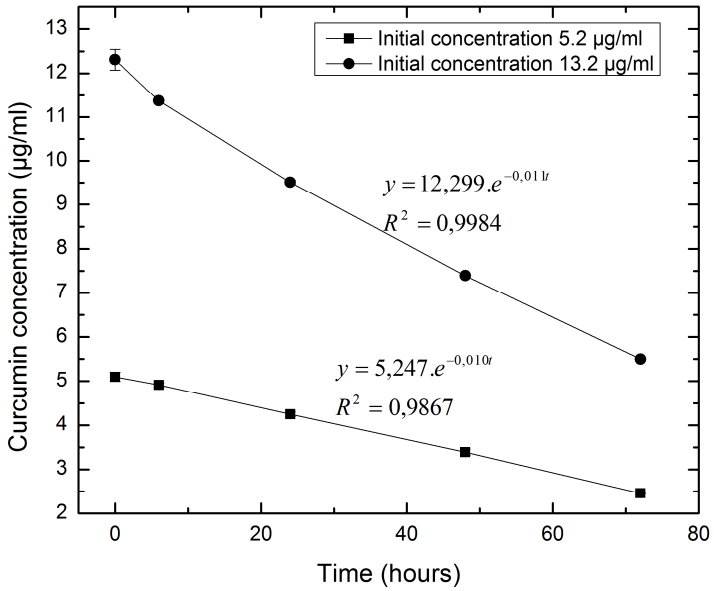


**Figure S1.** Kinetics of free curcumin degradation in PBS, SDS and ascorbic acid (respectively at 10mM, 50mM and 25µM) at 37°C

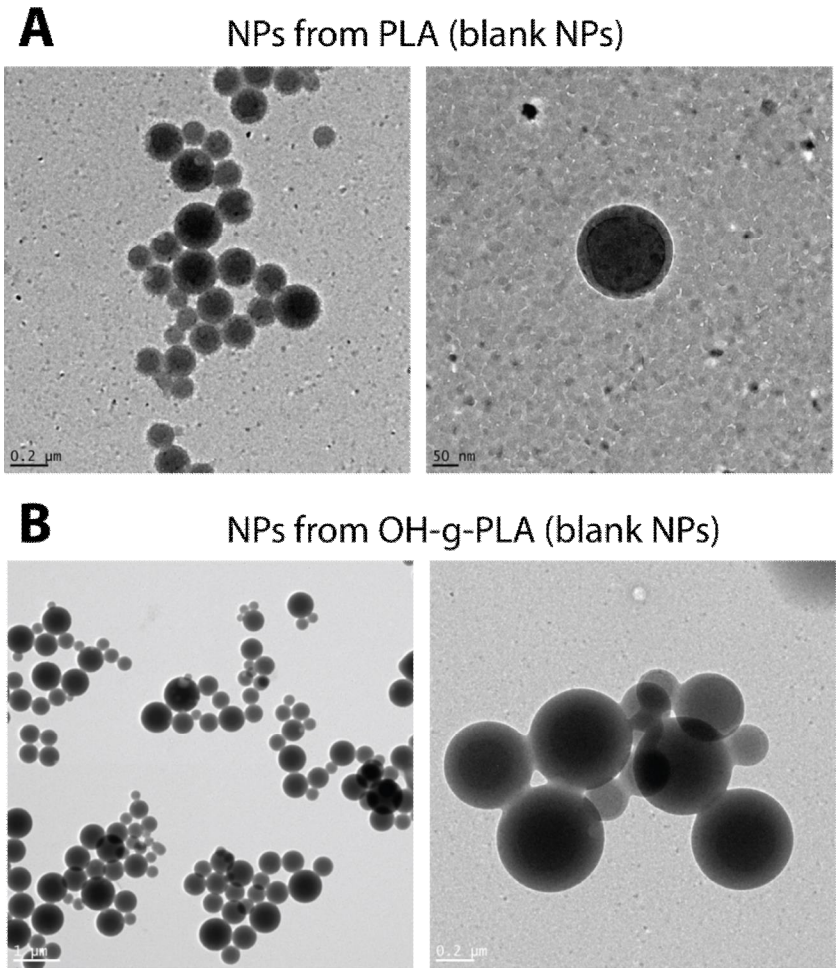


**Figure S2.** Cryo-TEM images of (A) NPs made from PLA (17 kD) and (B) from OH-*g*-PLA (see table 1 for structural information). Cryo-TEM image acquisition conditions are described in Material and Methods and are identical to the conditions used to generate images of PEGylated NPs displayed in Figure 3.

**Table S1.** Calculated modelling parameters for different NP batches

| *Polymer* | *Fitted Parameters* | | |
|---|---|---|---|
| | $K_d$ ($h^{-1}$) | $D$ ($\times 10^{-18}\ m^2.h^{-1}$) | $D$ ($\times 10^{-18}\ cm^2.s^{-1}$) |
| *PEG-PLA (6%)* | *0.009* | *63* | *175* |
| *PEG-8%g-PLA* | *0.01* | *75* | *208.3* |
| *PEG-12%g-PLA* | *0.01* | *110* | *305.6* |
| *PEG-15%g-PLA* | *0.008* | *18* | *50* |
| *PEG-20%g-PLA* | *0.008* | *3,5* | *9.7* |
| *PEG-26%g-PLA* | *0.01* | *6* | *16.7* |
| *PEG-38%g-PLA* | *0.011* | *10* | *27.8* |

**Table S2.** Curcumin physical properties
*(source: PubChem: http://pubchem.ncbi.nlm.nih.gov/)*

| **Parameters** | ***Values*** | ***Units*** |
|---|---|---|
| $M_w$ | 368.38 | $g.mol^{-1}$ |
| Melting point | 183 | $^oC$ |
| Pka | 7.8; 8.5; 9.0 | |
| Water solubility | 3.12 | $mg.l^{-1}$ |
| PBS 10 mM, 7.4 solubility * | $2.99\ 10^{-8}$ | $mol.l^{-1}$ |
| Log P | 3.47 | |

** from reference [1]*

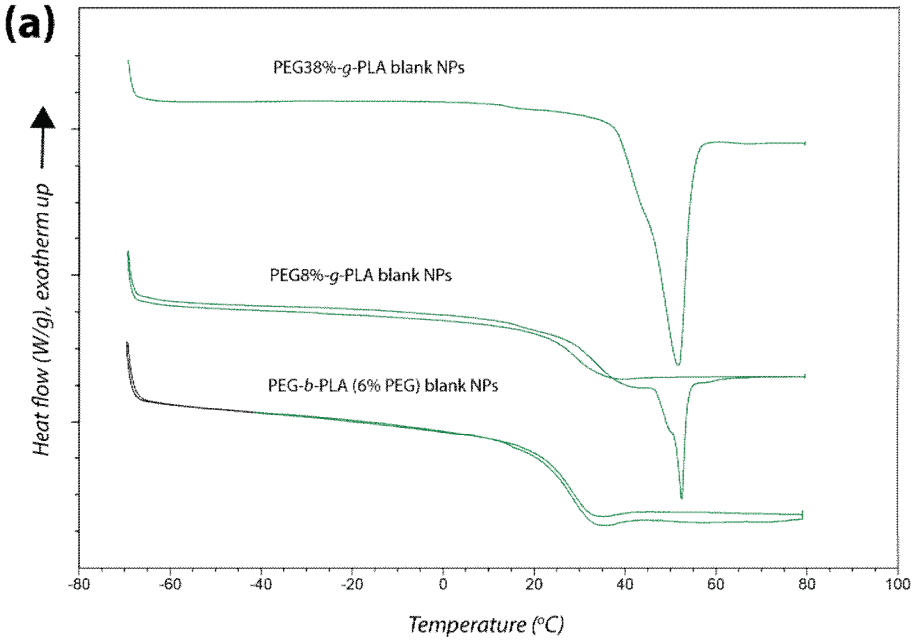

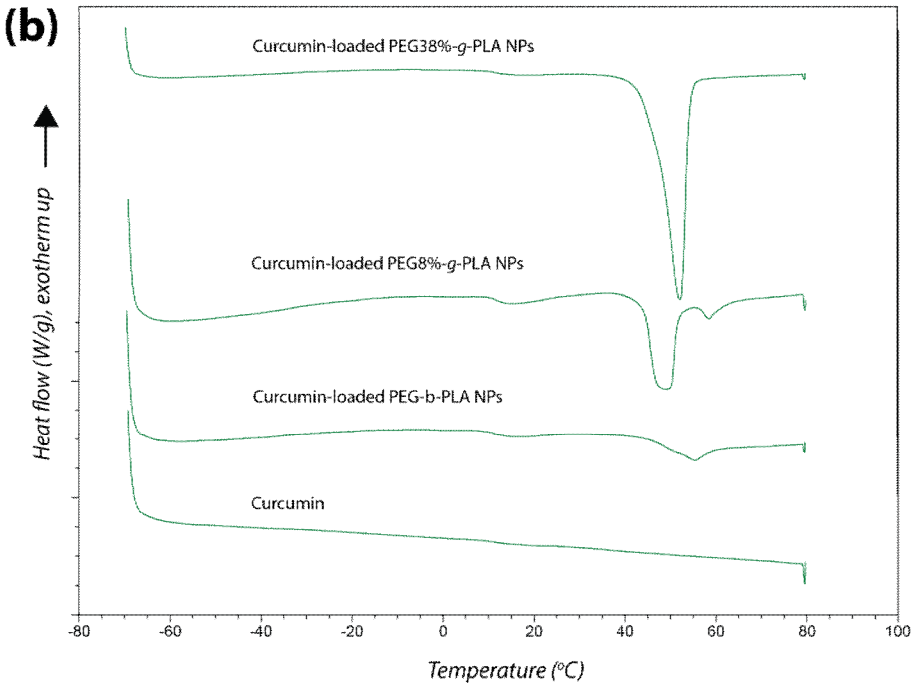


**Figure S3.** DSC thermograms, of blank (a) and curcumin-loaded NPs (b), showing effect of curcumin encapsulation on polymer thermal properties.

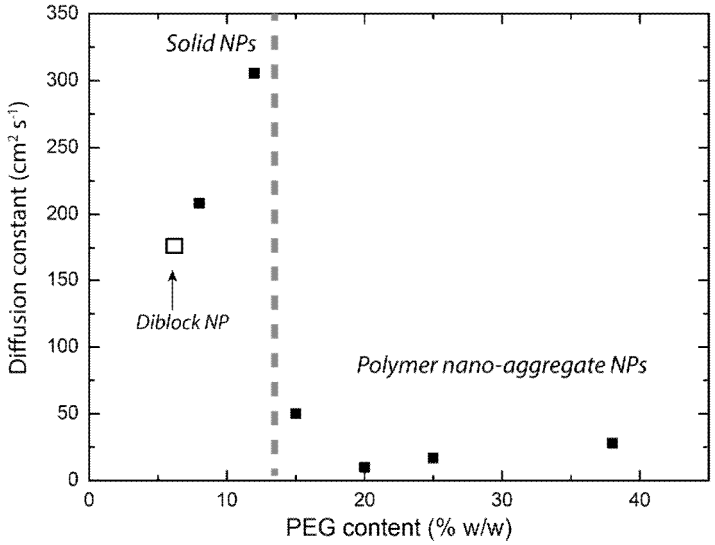


**Figure S4.** Curcumin diffusion constant as a function of polymer PEG content (% w/w).

**REFERENCE**

1. Letchford, K.; Liggins, R.; Burt, H., Solubilization of hydrophobic drugs by methoxy poly(ethylene glycol)-block-polycaprolactone diblock copolymer micelles: Theoretical and experimental data and correlations. *J. Pharm. Sci.* **2008,** 97, (3), 1179-1190.